Role of the hydrophobic and charged residues in the 218–226 region of apoA-I in the biogenesis of HDL[1]

Panagiotis Fotakis,*,† Andreas K. Kateifides,*,† Christina Gkolfinopoulou,§ Dimitra Georgiadou,§ Melissa Beck,*,† Katharina Gründler,* Angeliki Chroni,§ Efstratios Stratikos,§ Dimitris Kardassis,† and Vassilis I. Zannis[2],*

Whitaker Cardiovascular Institute,* Boston University School of Medicine, Boston, MA 02118; Department of Biochemistry,† University of Crete Medical School, Heraklion, Crete, Greece 71110; and National Center for Scientific Research "Demokritos",§ Athens, Greece 15310

Abstract **We investigated the significance of hydrophobic and charged residues 218–226 on the structure and functions of apoA-I and their contribution to the biogenesis of HDL. Adenovirus-mediated gene transfer of apoA-I[L218A/L219A/V221A/L222A] in apoA-I$^{-/-}$ mice decreased plasma cholesterol and apoA-I levels to 15% of wild-type (WT) control mice and generated pre-β- and α4-HDL particles. In apoA-I$^{-/-}$ × apoE$^{-/-}$ mice, the same mutant formed few discoidal and pre-β-HDL particles that could not be converted to mature α-HDL particles by excess LCAT. Expression of the apoA-I[E223A/K226A] mutant in apoA-I$^{-/-}$ mice caused lesser but discrete alterations in the HDL phenotype. The apoA-I[218–222] and apoA-I[E223A/K226A] mutants had 20% and normal capacity, respectively, to promote ABCA1-mediated cholesterol efflux. Both mutants had ~65% of normal capacity to activate LCAT in vitro. Biophysical analyses suggested that both mutants affected in a distinct manner the structural integrity and plasticity of apoA-I that is necessary for normal functions. We conclude that the alteration of the hydrophobic 218–222 residues of apoA-I disrupts apoA-I/ABCA1 interactions and promotes the generation of defective pre-β particles that fail to mature into α-HDL subpopulations, thus resulting in low plasma apoA-I and HDL. Alterations of the charged 223, 226 residues caused milder but discrete changes in HDL phenotype.—** Fotakis, P., A. K. Kateifides, C. Gkolfinopoulou, D. Georgiadou, M. Beck, K. Gründler, A. Chroni, E. Stratikos, D. Kardassis, and V. I. Zannis. **Role of the hydrophobic and charged residues in the 218–226 region of apoA-I in the biogenesis of HDL.** ***J. Lipid Res.*** 54: **3281–3292.**

Supplementary key words apolipoprotein A-I mutations • pre-β and α-HDL particles • dyslipidemia • LCAT

ApoA-I is the major protein component of HDL and plays an essential role in the biogenesis, maturation, and the functions of HDL (1–3). The biogenesis and remodeling of HDL occurs extracellularly and requires ABCA1, LCAT, and several other proteins (4). HDL biogenesis occurs predominantly in the liver and, to a lesser extent, in extrahepatic tissues (5, 6). The crucial role of apoA-I, ABCA1, and LCAT for the biogenesis of HDL has been established by naturally occurring mutations in these proteins in humans with low HDL levels (7–9).

In previous studies, systematic mutagenesis and gene transfer of human apoA-I mutants in apoA-I-deficient (apoA-I$^{-/-}$) mice disrupted specific steps along the pathway of the biogenesis of HDL and generated discrete lipid and lipoprotein phenotypes (10). The phenotypes generated included inhibition of the formation of HDL (1); generation of unstable intermediates (11, 12); inhibition of the activation of LCAT (13); and increase in plasma cholesterol or increase in both plasma cholesterol and triglycerides (14). The previous studies also showed that apoA-I-deletion mutants that lack residues 220–231 have diminished capacity to promote ABCA1-mediated cholesterol efflux and fail to cross-link with ABCA1 and to synthesize spherical HDL (1, 15)

In the present study, we investigated the role of four hydrophobic (L218, L219, V221, L222) and two charged

This work was supported by National Institutes of Health Grant HL-48739, General Secretariat of Research and Technology of Greece Grant Synergasia 09SYN-12-897 (to D.K. and A.C.), and Ministry of Education of Greece Grant Thalis MIS 377286 (to D.K., A.C., and E.S.). D. Georgiadou was supported by the graduate fellowship program of the National Center for Scientific Research Demokritos. P. Fotakis has been supported by pre-doctoral training Fellowship HERACLEITUS II by the European Union and Greek national funds through the Operational Program "Education and Lifelong Learning" of the National Strategic Reference Framework (NSRF).

Manuscript received 28 March 2013 and in revised form 27 August 2013.

Published, JLR Papers in Press, August 29, 2013
DOI 10.1194/jlr.M038356

Abbreviations: ANS, 8-anilino-1-naphthalene-sulfonate; apoA-I[218–222], the apoA-I carrying the L218A/L219A/V221A/L222A mutations; apoA-I[E223A/K226A], the apoA-I carrying the E223A/K226A mutations apoA-I$^{-/-}$, apoA-I-deficient; apoA-I$^{-/-}$ × apoE$^{-/-}$, apoA-I and apoE double-deficient; CD, circular dichroism; cpt-cAMP, 8-(4-chlorophenylthio) adenosine 3′:5′-cyclic monophosphatase; DMPC, dimyristoyl-L-α-phosphatidylcholine; EM, electron microscopy; FPLC, fast-protein liquid chromatography; GdnHCl, guanidine hydrochloride; HEK293, human embryonic kidney 293; HTB-13, SW 1783 human astrocytoma; pfu, plaque-forming unit; POPC, β-oleoyl-γ-palmitoyl-L-α-phosphatidylcholine; rHDL, reconstituted HDL; WMF, wavelength of maximum fluorescence; WT, wild-type.

[1] See referenced companion article, *J. Lipid Res.* 2013, 54: 3293–3302.

[2] To whom correspondence should be addressed.
e-mail: vzannis@bu.edu

[S] The online version of this article (available at http://www.jlr.org) contains supplementary data in the form of two tables, three figures, and methods.

(E223, K226) residues, located within or in the vicinity of the 220–231 region, on the biogenesis of HDL and the properties of apoA-I. The rationale for the alteration of these residues that reside within the 222–226 domain was based on the significance of this region for the structure of apoA-I. The crystal structure at 3.2 Å resolution of a truncated, lipid-free form of apoA-I [Δ(1–43)] that lacks the amino terminal domain indicated that, with the exception of the 220–227 region, apoA-I consists of a nearly continuous amphipathic α-helical sequence that is punctuated by small or pronounced kinks (16, 17). Most recently the three-dimensional structure of a dimeric truncated form of lipid-free apoA-I[Δ(185–243)] was determined at 2.2 A^o resolution (18). The structure showed that the N-terminal domain stabilizes the apoA-I dimer in solution and forces it to an antiparallel configuration that is similar to the configuration that the two apoA-I monomers assume when bound to discoidal HDL particles (16–19). In this configuration, it was proposed that the unstructured loop consisting of residues 220–227 allows helices 10 of each monomer to register in antiparallel orientation relative to the other.

In the present study, physicochemical studies and in vitro experiments determined how the mutations affected the structure of apoA-I and the ability of the mutant proteins to promote ABCA1-mediated cholesterol efflux and to activate LCAT. Adenovirus-mediated gene transfer of the apoA-I[218–222] mutant in apoA-$I^{-/-}$ × apoE$^{-/-}$ mice led to the formation of only pre-β-HDL particles and a small number of discoidal HDL particles. In contrast to previous studies (11–13), this defect, observed for the first time, could not be corrected by coexpression of the apoA-I[218–222] mutant and LCAT. Expression of the apoA-I[E223A/K226A] mutant in apoA-$I^{-/-}$ mice caused small alterations in the apoA-I structure and the HDL phenotype, suggesting that these residues also contribute to the efficient formation of HDL.

In addition to the drastic effect of the L218A/L219A/V221A/L222A mutations on the biogenesis of HDL, the mutants also inhibited the ability of lipid-free apoA-I to promote transendothelial transport (20), as well as its bactericidal activity against Gram-negative bacteria (21), indicating the importance of the 218–222 residues for the functions of apoA-I.

EXPERIMENTAL PROCEDURES

Materials

Materials not mentioned in this section have been obtained from sources described previously (2, 14).

Methods

Generation of adenoviruses expressing the wild-type and the mutant apoA-I forms and human LCAT. The apoA-I gene lacking the BglII restriction site that is present at nucleotide position 181 of the genomic sequence relative to the ATG codon of the gene was cloned into the pCDNA3.1 vector to generate the pCDNA3.1-apoA-I(ΔBglII) plasmid as described (12). This plasmid was used as a template to introduce the apoA-I mutations apoA-I[218–222] and apoA-I[E223A/K226A] using the QuickChange® XL mutagenesis kit (Stratagene, Santa Clara, CA) and the mutagenic primers shown in supplementary Table I. The recombinant adenoviruses were packaged in 911 cells, amplified in human embryonic kidney 293 (HEK293) cells, purified, and titrated as described (12).

The human LCAT cDNA in the pENTR221 vector was a gift of Dr. J. A. Kuivenhoven (University of Amsterdam). The LCAT cDNA was amplified using primers that contained restriction sites for BglII and EcoRV, respectively, at the 5′ and 3′ ends, as shown in supplementary Table I. The LCAT cDNA was digested with BglII and EcoRV and cloned into the corresponding sites of the pAdTrack-CMV vector. The recombinant adenovirus was constructed, purified, and titrated as described (12).

ApoA-I production, purification, and use for functional and physicochemical studies. Wild-type (WT) apoA-I, apoA-I[218–222] mutant, and apoA-I[E223A/K226A] mutant protein were obtained from the culture media of HTB-13 cells grown in roller bottles following infection with adenoviruses expressing the corresponding proteins. For protein production, the culture medium was collected every 24 h, dialyzed against 25 mM ammonium bicarbonate, and lyophilized. For the purification of WT apoA-I and apoA-I[E223A/K226A] mutant, the lyophilized medium was resuspended in 0.01M Tris (pH 8), filtered, and passed through a 5 ml HiTrap Q HP column (GE Healthcare). The proteins were eluted with linear gradient of 1M NH_4CO_3 in the Tris buffer, as described previously (1). The apoA-I[218–222] mutant was purified with the same procedure under denaturing conditions (8M urea) to facilitate the dissociation of apoA-I from other proteins that coelute with mutant apoA-I under native conditions. The purity of the apoA-I preparation was assessed by SDS-PAGE, and fractions greater than 95% pure were pooled.

ABCA1-dependent cholesterol efflux and LCAT assays. ABCA1-dependent efflux of cholesterol was measured in cultures of J774 macrophages in which expression of ABCA1 was induced by a cAMP analog using WT and mutant apoA-I forms as cholesterol acceptors. The J774 mouse macrophages were labeled with 0.3 μCi/ml [^{14}C]cholesterol ([4-^{14}C]cholesterol, 0.04 mCi/ml of specific activity 50 mCi/mmol; Perkin-Elmer Life Sciences) for 24 h and then treated with 0.3 mM cpt-cAMP [8-(4-chlorophenylthio)-cAMP] for 24 h. Cholesterol efflux was determined as described previously (1).

LCAT was purified as described (14) from the culture medium of human HTB13 cells infected with an adenovirus expressing the human LCAT cDNA (22). The reconstituted HDL (rHDL) particles used as the substrate contained cholesterol, and [^{14}C] cholesterol, β-oleoyl-γ-palmitoyl-L-α-phosphatidylcholine (POPC), and apoA-I. rHDL was prepared by the sodium cholate dialysis method as described previously (23). rHDL particles without ^{14}C-cholesterol containing mutant forms of apoA-I were prepared with the same procedure to measure their size by electron microscopy (EM). The size of these particles was determined from the negatives of the EM images. The enzymatic reactions and the derivation of the apparent V_{max} and K_m were carried out as described previously (13).

Physicochemical measurements. Derivation of far-UV spectra, thermal and chemical denaturation profiles, and 8-anilino-1-naphthalene-sulfonate (ANS) fluorescence spectra of the WT apoA-I, apoA-I[218–222] mutant, and apoA-I[E223A/K226A] mutant are described in the supplementary methods.

Animal studies. ApoA-$I^{-/-}$ (ApoA1^{tm1Unc}) C57BL/6J mice (24) were purchased from Jackson Laboratories (Bar Harbor,

ME). Mice deficient for apoA-I$^{-/-}$ and apoE$^{-/-}$ were a gift of Dr. Fayanne Thorngate and Dr. David Williams (25) or were obtained by crossing apoA-I$^{-/-}$ with apoE$^{-/-}$ (26). The mice were maintained on a 12 h light/dark cycle and standard rodent chow. All procedures performed on the mice were in accordance with National Institutes of Health guidelines and followed a protocol (AN-14219.2012.10) approved by the Institutional Animal Care and Use Committee (IACUC). ApoA-I$^{-/-}$ or apoA-I$^{-/-}$ × apoE$^{-/-}$ mice, 6–8 weeks of age, were injected via the tail vein with 1–2 × 10^9 pfu of recombinant adenovirus per animal. The animals were euthanized four days after injection following a four-hour fast. Five to six mice were used for each set of experiments. Determination of plasma lipids and apoA-I levels, fractionation of plasma by fast-protein liquid chromatography (FPLC), and density gradient ultracentrifugation EM of HDL and two-dimensional gel electrophoresis of plasma are as described (1, 2, 27 and supplementary methods).

Statistics. Statistical analyses were performed by two-tailed Student *t*-test with equal variance.

RESULTS

Expression of the apoA-I transgene following adenovirus infection

Total hepatic RNA was isolated from the livers of apoA-I$^{-/-}$ four days after infection with adenoviruses expressing the WT apoA-I, apoA-I[218–222] mutant, and apoA-I [E223A/K226A] mutant. The relative expression of the WT and the mutant apoA-I transgenes was determined by qPCR as described in the Experimental Procedures. This analysis showed that the expression of WT and the apoA-I [218–222] mutant were comparable, whereas the expression of apoA-I[E223A/K226A] was approximately 165% of that of WT apoA-I (supplementary Table II).

Plasma lipid and apoA-I levels and FPLC profiles

Plasma lipids and apoA-I were determined four days after infection of apoA-I$^{-/-}$ mice with adenoviruses expressing the WT and the two apoA-I mutants. It was found that the apoA-I[218–222] mutant decreased plasma cholesterol and apoA-I levels to approximately 15% as compared with WT apoA-I. The plasma apoA-I levels of the apoA-I[E223A/K226A] mutant were not statistically different from those of WT apoA-I, whereas the plasma cholesterol levels were significantly lower (62% as compared with WT apoA-I) (**Fig. 1A**, B). The plasma triglycerides of the apoA-I[E223A/K226A] mutant were slightly increased as compared with wild-type apoA-I ($P < 0.05$) (supplementary Table II). FPLC analysis of plasma from apoA-I$^{-/-}$ mice infected with the recombinant adenovirus expressing either WT apoA-I or the two apoA-I mutants showed that in all cases cholesterol was distributed in the HDL region and that the HDL cholesterol peak of the apoA-I[218–222] mutant was greatly diminished (Fig. 1C).

Fractionation of plasma, EM analysis, and two-dimensional electrophoresis of plasma of apoA-I$^{-/-}$ mice expressing the WT and the mutant forms of apoA-I

Fractionation of plasma by density gradient ultracentrifugation and subsequent analysis of the resulting fractions by SDS-PAGE showed that the WT apoA-I was equally distributed in the HDL2 and HDL3 region and that the apoA-I[E223A/K226A] and apoA-I[218–222] mutants were predominantly distributed in the HDL3 and, to a lesser extent, the HDL2 region (**Fig. 2A**, B). The apoA-I[218–222] mutant was characterized by low levels of apoA-I and increased levels of mouse apoE that floated in the HDL2/HDL3 (Fig. 2C and supplementary Fig. I-A, B) and in the VLDL/IDL/LDL region.

Analysis of the HDL fractions 6 and 7 obtained following density gradient ultracentrifugation by EM showed that the WT apoA-I as well as the two apoA-I mutants (apoA-I[E223A/K222A] and apoA-I[218–222]) generated spherical particles (Fig. 2D–F). Two-dimensional gel electrophoresis of plasma showed that WT apoA-I formed normal pre-β- and α-HDL subpopulations (Fig. 2G); the apoA-I[E223A/K226A] mutant formed predominantly α2, α3, and α4 and had increased amount of pre-β subpopulations (Fig. 2H); and the apoA-I[218–222] mutant formed only pre-β, α4, and α3 subpopulations (Fig. 2I).

To clarify whether the HDL particles observed in Fig. 2F originate from the apoA-I[218–222] mutant or mouse apoE that float in the HDL region (Fig. 2C and supplementary Fig. I-A, B), we performed adenovirus-mediated gene transfer in apoA-I$^{-/-}$ × apoE$^{-/-}$ mice, which lack both mouse apoA-I and apoE. Analysis of relative expression of the WT and the mutant apoA-I transgenes by qPCR showed that the expression of WT apoA-I and apoA-I[218–222] mutant were comparable (supplementary Table II). Separation of the plasma by density gradient ultracentrifugation and SDS-PAGE analysis of the fractions showed that WT apoA-I was distributed predominantly in the HDL2/HDL3 region (**Fig. 3A**). EM analysis of the fractions 6 and 7 obtained by density gradient ultracentrifugation of the plasma showed that WT apoA-I generated spherical particles (Fig. 3B). Two-dimensional gel electrophoresis showed that the plasma of mice expressing WT apoA-I contained the normal pre-β- and α-HDL subpopulations (Fig. 3C). SDS-PAGE analysis of plasma fractions obtained from mice expressing the apoA-I[218–222] mutant showed the presence of small amounts of the mutant protein in the HDL3 region (Fig. 3D). The L218A/L219A/V221A/L222A mutations in apoA-I resulted in a great increase in plasma apoA-IV that floated in the IDL/LDL/HDL2/HDL3 region (Fig. 3D and supplementary Fig. II) and the presence of apoB-48 in the HDL region (Fig. 3E). The apoA-I[218–222] mutant generated few discoidal particles as well as particles corresponding in size to VLDL (48.5 ± 15 nm), IDL (28.8 ± 3 nm), and LDL (20.2 ± 2.5 nm) (Fig. 3F). The appearance of the LDL- and IDL-sized particles is also supported by the presence of apoB-48 in fractions 6 and 7 used for the EM analysis (Fig. 3E). The plasma of mice expressing the apoA-I[218–222] mutant contained only pre-β-HDL particles (Fig. 3G). The relative migration of the particles generated by WT apoA-I and the apoA-I[218–222] mutant was established by two-dimensional gel electrophoresis of mixtures of the plasmas containing these two apoA-I forms (Fig. 3H).

Previous studies have shown that the low HDL levels and the abnormal HDL phenotypes of some natural apoA-I

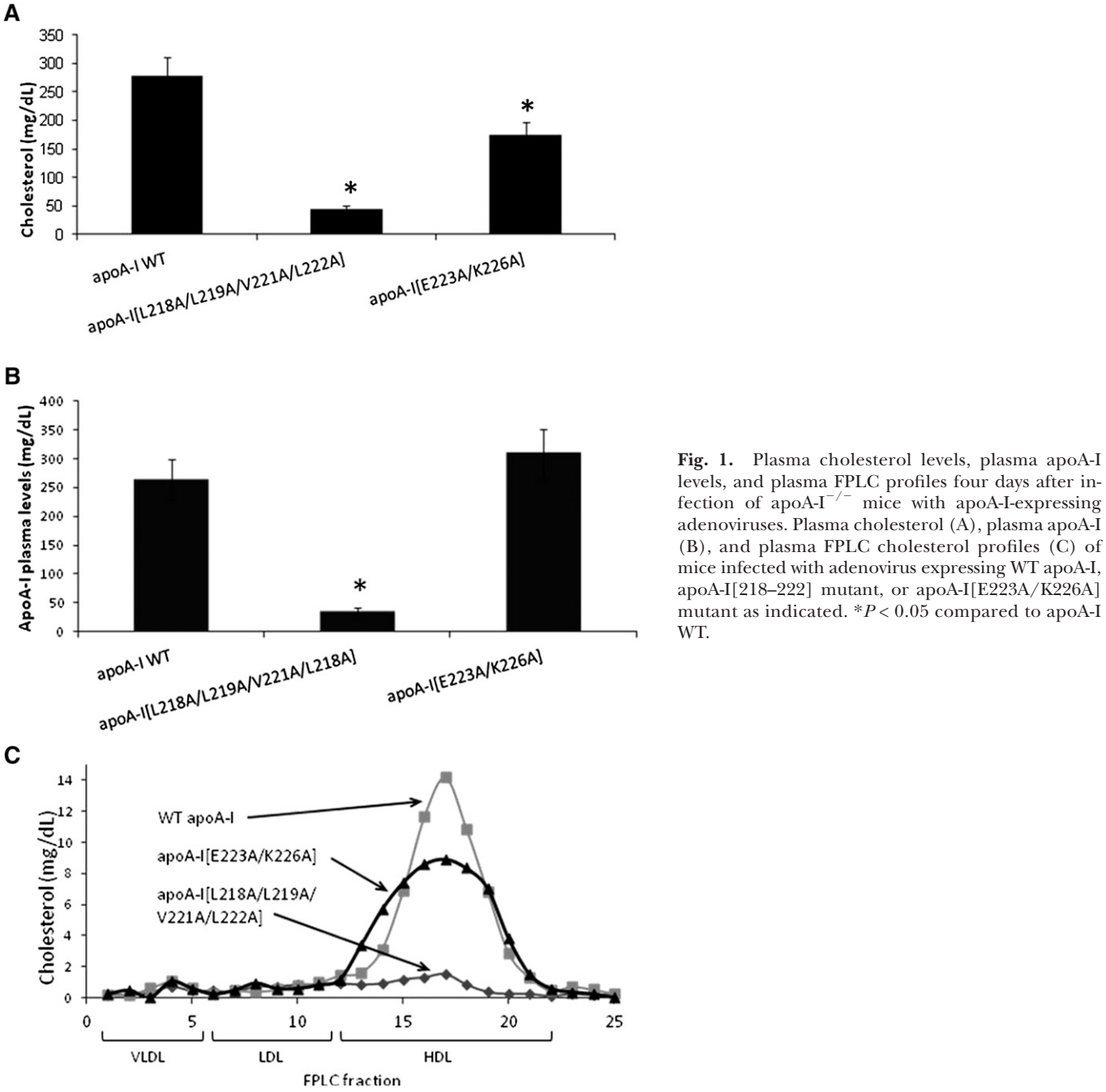

Fig. 1. Plasma cholesterol levels, plasma apoA-I levels, and plasma FPLC profiles four days after infection of apoA-I$^{-/-}$ mice with apoA-I-expressing adenoviruses. Plasma cholesterol (A), plasma apoA-I (B), and plasma FPLC cholesterol profiles (C) of mice infected with adenovirus expressing WT apoA-I, apoA-I[218–222] mutant, or apoA-I[E223A/K226A] mutant as indicated. *$P < 0.05$ compared to apoA-I WT.

mutants could be corrected by excess LCAT (11–13). To assess the potential insufficiency of LCAT that led to the generation of discoidal particles observed in Fig. 3F, we carried out gene transfer of both the apoA-I[218–222] mutant and LCAT in apoA-I$^{-/-}$ × apoE$^{-/-}$ mice. The lipid parameters and the expression levels of the transgene are shown in supplementary Table II. The FPLC profiles of plasma obtained from mice expressing WT apoA-I, apoA-I[218–222] mutant, or apoA-I[218–222] mutant in the presence of LCAT are shown in **Fig. 4A**. This comparative analysis showed that in all cases the great majority of cholesterol was distributed in the VLDL/IDL region. In the case of WT apoA-I, a small amount of cholesterol was distributed in the HDL region, whereas the apoA-I[218–222] mutant did not have an HDL cholesterol peak (Fig. 4A). Coexpression of the apoA-I[218–222] mutant and LCAT had a small effect on the HDL cholesterol peak, but it generated a pronounced cholesterol shoulder in the VLDL/IDL/LDL region (Fig. 4A). Density gradient ultracentrifugation of plasma followed by SDS-PAGE analysis of the fractions showed that a small amount of the mutant apoA-I was found in the HDL3. In addition, the plasma concentration of mouse apoA-IV increased, and the protein shifted toward the VLDL/IDL/LDL region (Fig. 4B). EM analysis of the HDL fraction obtained by density gradient ultracentrifugation showed the presence of small number of spherical HDL particles, along with larger particles corresponding in size to LDL and IDL (Fig. 4C). The appearance

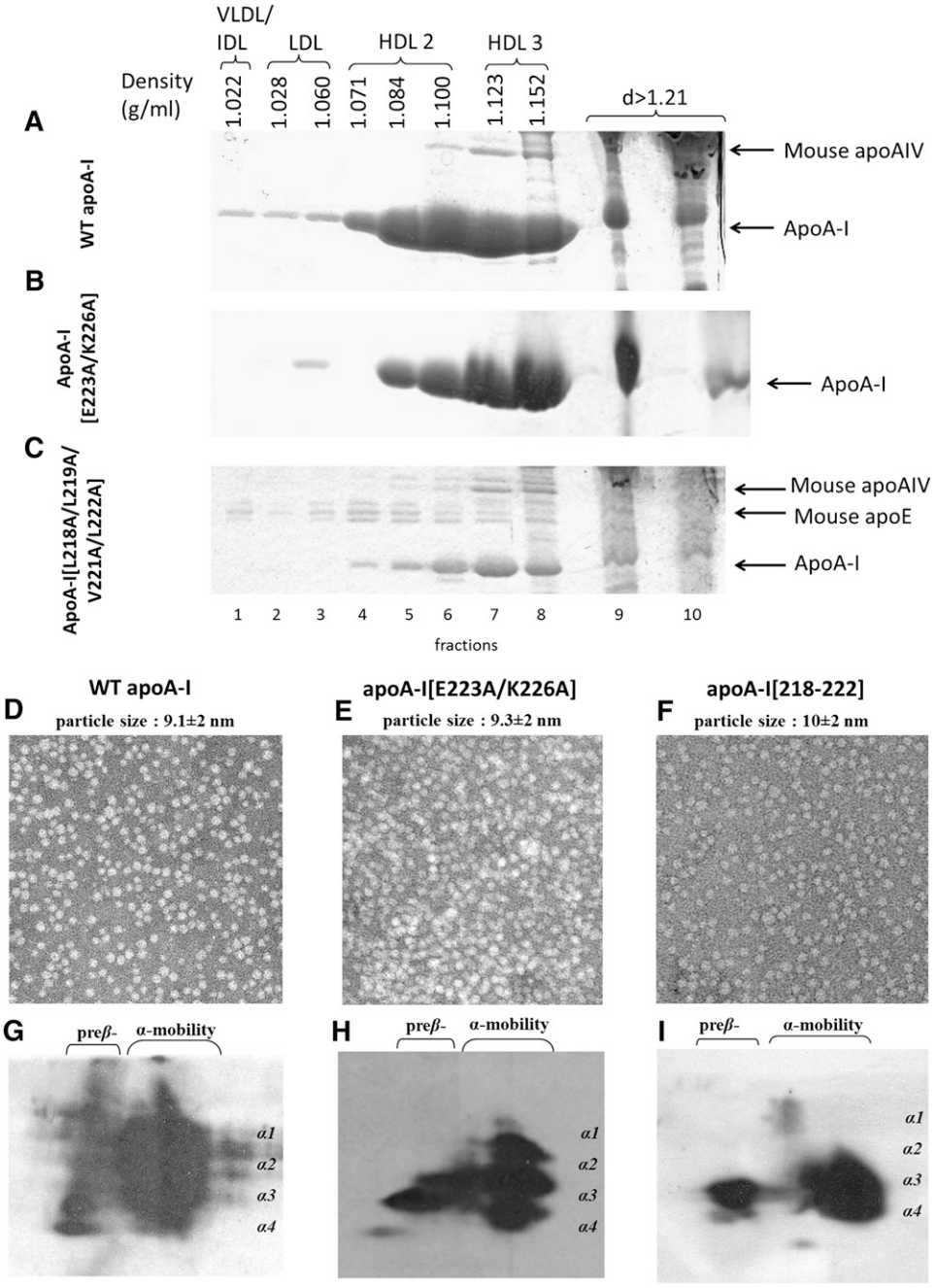

Fig. 2. Analysis of plasma of apoA-I$^{-/-}$ mice infected with adenoviruses expressing the WT apoA-I (A), apoA-I[E223A/K226A] mutant (B), or the apoA-I[218–222] mutant (C) by density gradient ultracentrifugation and SDS-PAGE. EM analysis of HDL fractions 6 and 7 obtained from apoA-I$^{-/-}$ mice expressing the WT apoA-I (D), the apoA-I[E223A/K226A] mutant (E), or the apoA-I[218–222] mutant (F) following density gradient ultracentrifugation of plasma. The photomicrographs were taken at 75,000× magnification and enlarged three times. Two-dimensional gel electrophoresis of plasma of apoA-I$^{-/-}$ mice infected with adenoviruses expressing the WT apoA-I (G), the apoA-I[E223A/K226A] mutant (H), and the apoA-I[218–222] mutant (I).

of the LDL- and IDL-sized particles is also supported by the presence of apoB-48 in fractions 6 and 7 used for the EM analysis (Fig. 4D). It is possible that the LDL- and IDL-sized particles might arise by initial formation of apoA-IV-containing HDL (28) and subsequent fusion of such HDL particles with apoB-containing lipoproteins (Fig. 4C, D). Two-dimensional gel electrophoresis showed that the plasma of mice coexpressing the apoA-I[218–222] mutant and LCAT contained only small amount of pre-β- and α4-HDL particles (Fig. 4E).

Comparative analysis of the in vitro functions of WT apoA-I, apoA-I[218–222] mutant, and apoA-I[E223A/K226A] mutant

The secretion of WT and mutant forms of apoA-I in the culture medium of HTB-13 cells following infection of the

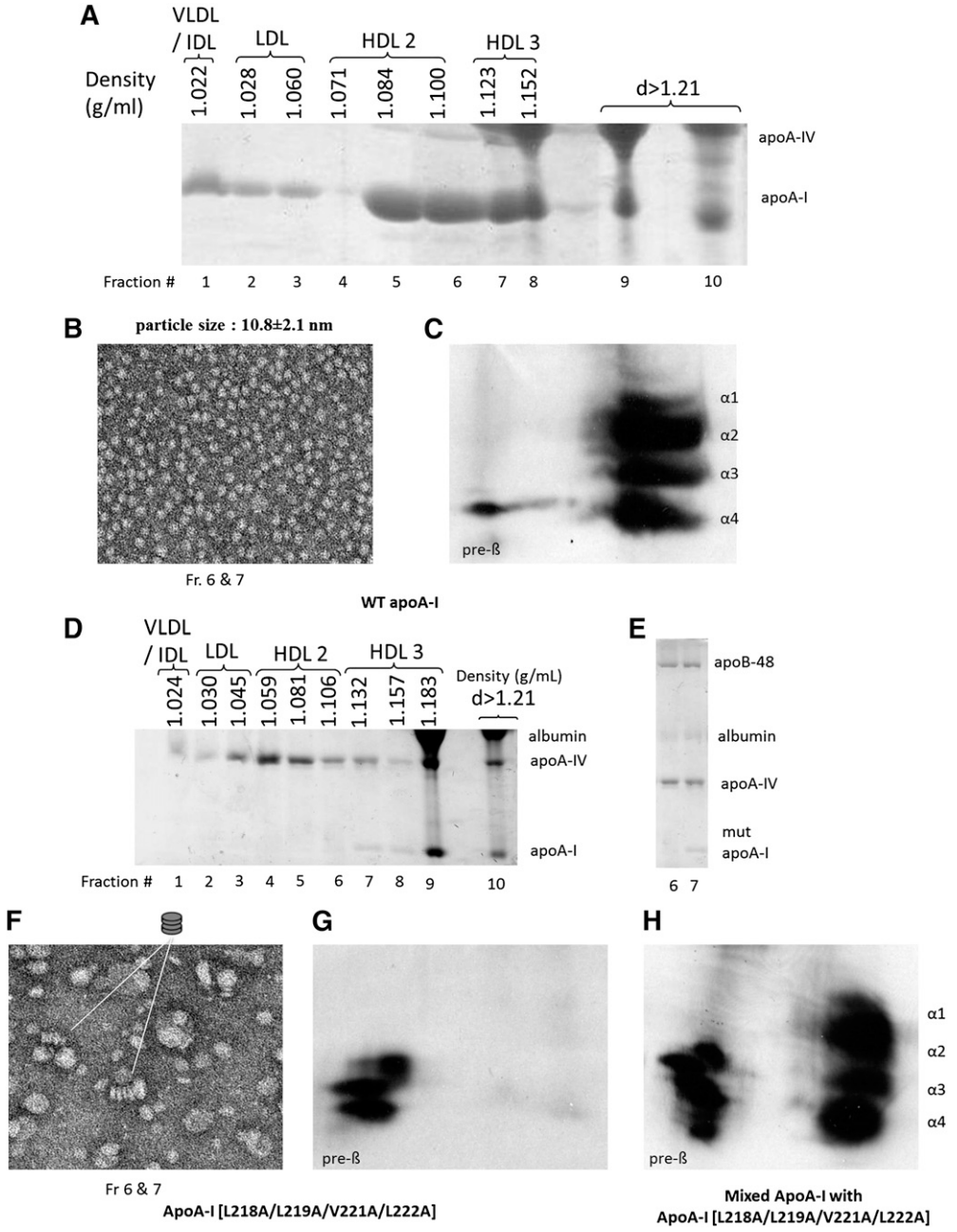

Fig. 3. Analysis of plasma of apoA-I$^{-/-}$ × apoE$^{-/-}$ mice infected with adenoviruses expressing WT apoA-I (A) or apoA-I[218–222] mutant (D) by density gradient ultracentrifugation and SDS-PAGE. EM analysis of HDL fractions 6 and 7 obtained from apoA-I$^{-/-}$ × apoE$^{-/-}$ mice expressing the WT apoA-I (B) or apoA-I[218–222] mutant (F) following density gradient ultracentrifugation of plasma as indicated. The photomicrographs were taken at 75,000× magnification and enlarged three times. E: SDS gel electrophoresis showing lipoprotein composition of fractions 6 and 7. These fractions were used for EM analysis in F. Two-dimensional gel electrophoresis of plasma of apoA-I$^{-/-}$ × apoE$^{-/-}$ mice infected with adenoviruses expressing WT apoA-I (C), apoA-I[L218–222] mutant (G), or mixture of samples obtained from mice expressing WT apoA-I and apoA-I[218–222] mutant (H).

cells with recombinant adenoviruses expressing the corresponding proteins was assessed as described previously (29). This analysis showed that the apoA-I[218–222] and apoA-I[E223A/K226A] mutants were secreted at comparable levels in the culture medium of the adenovirus-infected cells. To interpret the observed defects in HDL biogenesis that resulted from the apoA-I mutations, we purified WT apoA-I, as well as the apoA-I[218–222] and the apoA-I[E223A/K226A] mutants, from the culture media of HTB-13 cells grown in roller bottles and studied their properties in vitro. It was found that the ability of the apoA-I[218–222] mutant to promote ABCA1-mediated cholesterol efflux and to activate LCAT, were 20% and 66%, respectively, as compared with the WT control. The ability of the apoA-I[E223A/K226A] mutant to promote ABCA1-mediated cholesterol efflux was slightly increased

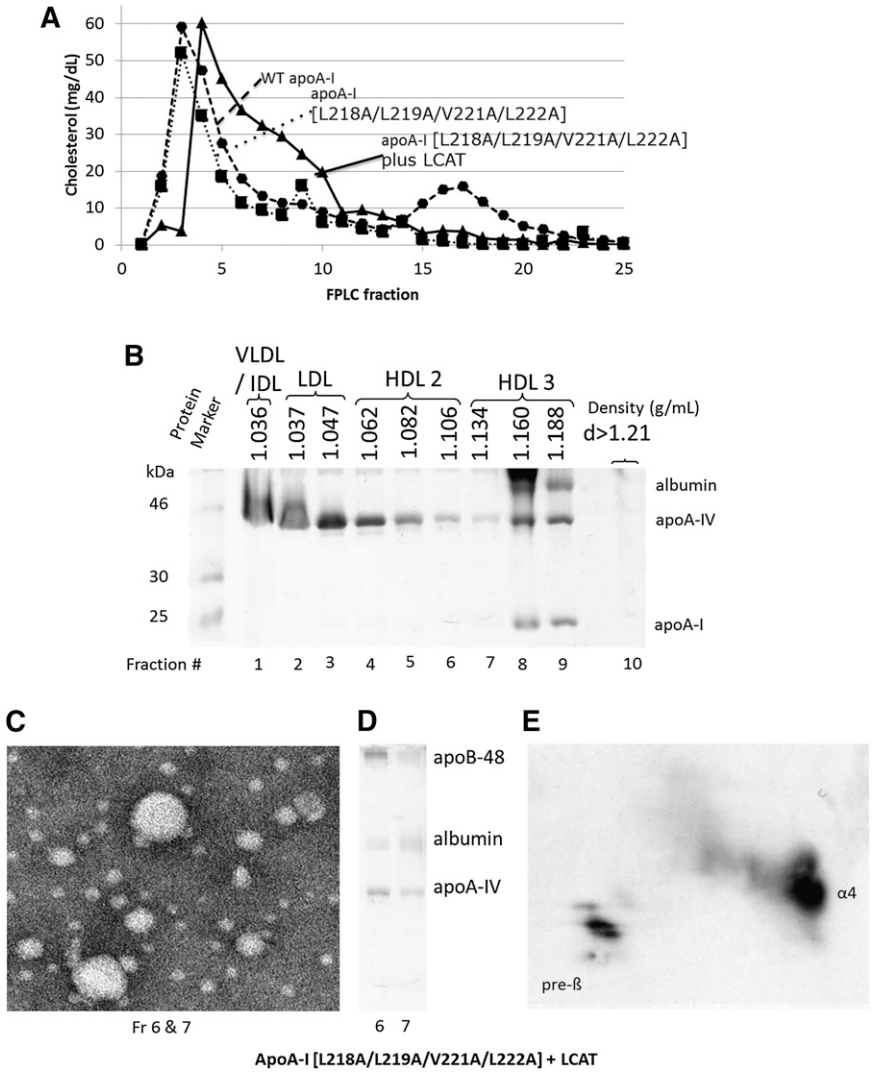

Fig. 4. Analyses of plasma of apoA-I$^{-/-}$ × apoE$^{-/-}$ mice infected with adenoviruses expressing the WT apoA-I or the apoA-I[218–222] mutant alone or in combination with human LCAT. A: Plasma FPLC profiles of mice expressing WT apoA-I or the apoA-I[218–222] mutant alone or in combination with LCAT as indicated. B: SDS-PAGE of fractions obtained by density gradient ultracentrifugation from mice expressing the apoA-I[218–222] mutant and LCAT. C: EM analysis of the HDL corresponding to fractions 6 and 7 of B. D: The photomicrograph was taken at 75,000× magnification and enlarged three times. SDS gel electrophoresis showing apolipoprotein composition of fractions 6 and 7 used for EM analysis in C. E: Two-dimensional gel electrophoresis of plasma of apoA-I$^{-/-}$ × apoE$^{-/-}$ mice infected with adenoviruses expressing the apoA-I[218–222] mutant and LCAT.

compared with that of WT apoA-I, and its ability to activate LCAT was 65% of the WT control (**Fig. 5A**, B).

Effect of the L218A/L219A/V221A/L222A and E223A/K226A mutations on the α-helical content, thermal unfolding, chemical unfolding, and hydrophobic surface exposure of apoA-I

To test whether the functional changes of the two apoA-I mutants are accompanied by changes in the structure and conformation of the protein, we used an array of biophysical assays to evaluate the effects of these mutations (**Fig. 6**). Circular dichroism (CD) measurements indicated 7% and 4.2% loss of helical content for the apoA-I[218–222] mutant and the apoA-I[E223A/K226A] mutant, respectively (Fig. 6A and **Table 1**). Thermal unfolding of apoA-I followed by CD measurements showed that the apoA-I[218–222] mutant had a much more cooperative unfolding transition, indicating a more compact structure for this mutant protein, whereas the apoA-I[E223A/K226A] mutant had a slightly less cooperative unfolding transition, indicating a slightly less compact structure for this mutant (Fig. 6B and Table 1). The chemical unfolding profile of the apoA-I[218–222] mutant, probed by intrinsic tryptophan fluorescence, was identical to that of the WT protein, whereas the chemical unfolding of the apoA-I [E223A/K226A] mutant was less cooperative than the WT apoA-I (Fig. 6C and Table 1). Overall, the apoA-I[E223A/K226A] mutant appears to be thermodynamically destabilized and is quite distinct from the apoA-I[218–222] mutant. Finally, the ANS fluorescence measurements indicated

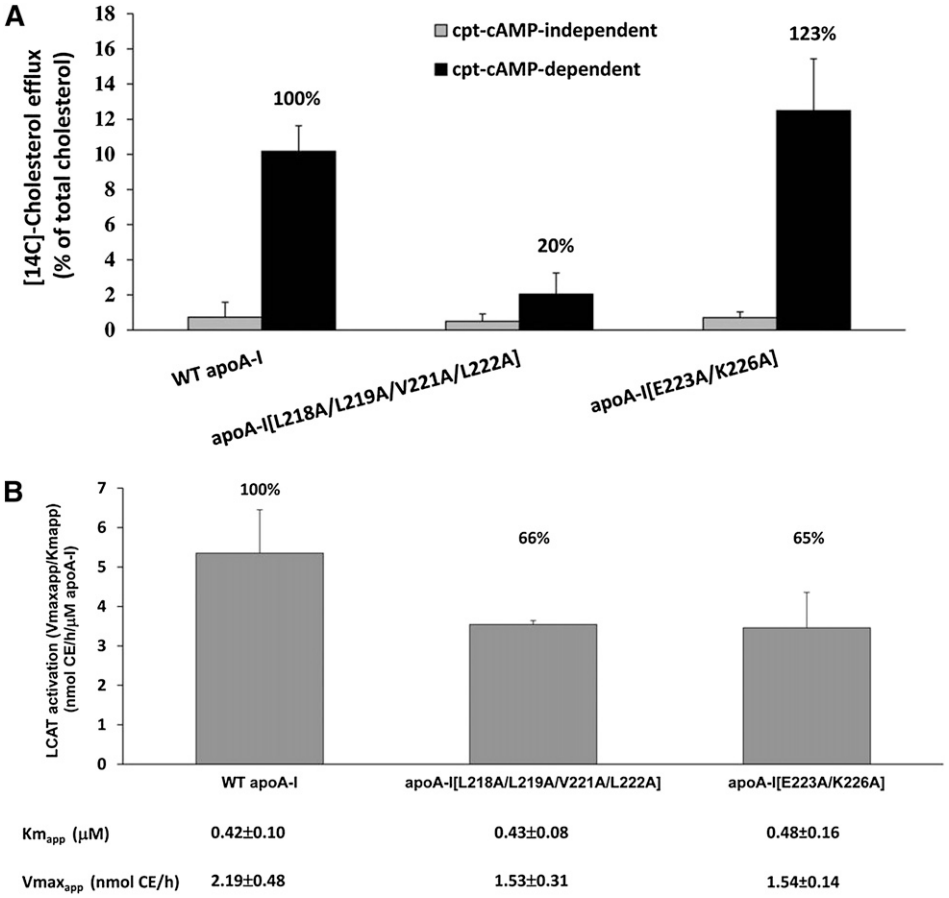

Fig. 5. A: ABCA1-mediated cholesterol efflux from J774 mouse macrophages treated with cpt-cAMP using WT apoA-I, apoA-I[218–222] mutant, and apoA-I[E223A/K226A] mutant as cholesterol acceptor. The ABCA1 independent and ABCA1-mediated efflux is shown. The ABCA1-mediated cholesterol efflux by WT apoA-I is set to 100%. B: LCAT activation capacity of WT apoA-I, apoA-I[218–222] mutant, and the apoA-I[E223A/K226A] mutant. Experiments were performed as described in the Experimental Procedures. The data represent the average from two independent experiments in triplicate.

that the apoA-I[218–222] mutant had a 40% reduction of hydrophobic surface exposure to the solvent, whereas the apoA-I[E223A/K226A] mutant had a 160% increase in the hydrophobic surface exposure to the solvent (Fig. 6D and Table 1).

DISCUSSION

Rationale for selection of the mutations

Lipid-free or minimally lipidated apoA-I promotes ABCA1-mediated cholesterol efflux and thus serves as an acceptor of cellular phospholipid and cholesterol (1, 30, 31). Lipid-bound apoA-I is a physiological activator of LCAT (31). The functional interactions between apoA-I and ABCA1 are important for cholesterol efflux and the biogenesis of HDL (1, 32, 33). To identify the specific C-terminal residues of apoA-I that are required for correct interactions with ABCA1 and/or LCAT that lead to the formation of mature α-HDL particles, we introduced two sets of mutations that span the 218–226 region of apoA-I. The properties of the apoA-I[218–222] and apoA-I[E223A/K226A] mutants thus generated were studied by in vitro experiments and adenovirus-mediated gene transfer.

L218A/L219A/V221A/L222A and E223A/K226A mutations alter the functional and physicochemical properties of apoA-I

The in vitro experiments showed that, compared with WT apoA-I, the capacity of the apoA-I[218–222] mutant to promote ABCA1-mediated cholesterol efflux and to activate LCAT was 20% and 66%, respectively. The capacity of the apoA-I[E223A/K226A] mutant to promote ABCA1-mediated cholesterol efflux was slightly increased compared with that of the WT control, and the capacity to activate LCAT was 65% of the WT control. The changes in the physicochemical properties of the apoA-I[218–222] mutant included a 7% decrease in its α-helical content, a more cooperative thermal unfolding transition (yet an identical chemical unfolding transition), and a 40% reduction of hydrophobic surfaces exposed to the solvent. The higher cooperativity observed during the thermal denaturation of this mutant suggests a more compact and stable structure, which may appear at odds with the lack of any observed stabilization during the chemical denaturation. The two methods, however, report on different aspects of the conformational change that follows protein denaturation (overall secondary structure versus

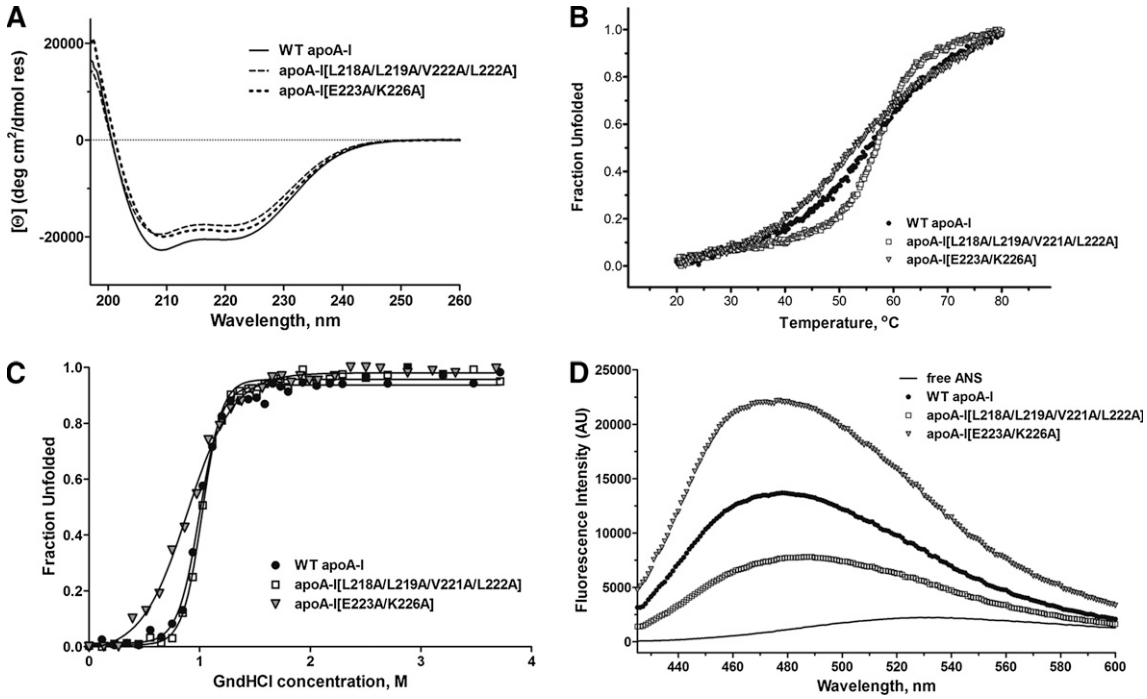

Fig. 6. Far-UV CD spectra of WT apoA-I, apoA-I[218–222] mutant, and apoA-I[E223A/K226A] mutant obtained at 25°C. A: Thermal denaturation profiles of WT apoA-I, apoA-I[218–222] mutant, and apoA-I[E223A/K226A] mutant determined by changes in molar ellipticity at 222 nm. B: Samples were denatured by increasing the temperature up to 80°C. Experimental points are depicted as dots. C: Chemical denaturation profile of WT apoA-I, apoA-I[218–222] mutant, and apoA-I[E223A/K226A] mutant. The intrinsic fluorescence signal of tryptophan of apoA-I was monitored while titrating with Gnd-HCl. The solid line represents nonlinear regression to a simple Boltzmann model. The experimental points are depicted as dots. D: ANS fluorescence spectra obtained in the presence of 50 μg/ml WT apoA-I, apoA-I[218–222] mutant, apoA-I[E223A/K226A] mutant, and buffer alone.

the immediate environment of the tryptophan residues). In apoA-I, all of the tryptophan residues are located in the N-terminal moiety of the molecule, and therefore, the lack of changes during chemical denaturation suggest that the thermodynamic stability of this domain is not affected by the mutation. Conversely, the altered thermal denaturation profile can be explained by localized changes in the folding and stability of the C-terminal moiety of the protein where the mutated residues are or to changes in the interactions between the C-terminal and N-terminal domain that primarily affect the stability of the C-terminal domain. However, since the two methods of denaturation use different mechanisms to unfold the protein, the possibility that the stabilization seen during

TABLE 1. Calculated biophysical parameters for WT and mutant apoA-I forms

Mutation	Circular Dichroism		Thermal Denaturation			Chemical Denaturation			ANS Binding
ApoA-I	α-Helix	T_m (°C)	Slope	Cooperativity Index (n)	ΔH (kcal/mol)	ΔG_D^o (kcal/mol)	$D_{1/2}$ (M)	m^c (kcal mol^{-2})	Fold Increase[a]
WT	60.0 ± 1.5	55.6 ± 0.4	8.3 ± 0.4	6.4 ± 0.2	25.9 ± 1.5	6.3 ± 0.4	1.01 ± 0.02	6.3 ± 0.4	6.0 ± 0.4
L218A/L219A/V221A/L222A	52.7 ± 1.6[b]	56.1 ± 0.8	4.6 ± 0.2[b]	9.7 ± 0.6[b]	46.4 ± 2.4[b]	6.6 ± 0.4	1.00 ± 0.03	6.4 ± 0.4	3.5 ± 0.2[b]
E223A/K226A	55.8 ± 1.1[c]	53.4 ± 0.2[b]	10.4 ± 1.4[d]	5.3 ± 0.7[b]	21.01 ± 2.2[e]	2.5 ± 0.2[b]	0.88 ± 0.02[f]	2.8 ± 0.1[b]	9.6 ± 0.5[b]

Values are means ± SD from three or four experiments. Parameters obtained from the indicated measurements are as follows: "α-helix" is the percentage of α-helical content of the protein as calculated from the molecular ellipticity of the protein sample at 222 nm; "T_m" is middle point of the thermal denaturation transition (melting temperature); "slope" is the calculated slope of the linear component of the thermal denaturation transition, around the melting temperature; "n" is an indicator of the cooperativity of the thermal unfolding transition and is calculated using the Hill equation n = (log 81) / log ($T_{0.9}$ / $T_{0.1}$), where $T_{0.9}$ and $T_{0.1}$ are the temperatures where the unfolding transition reaches a fractional completion of 0.9 and 0.1; "ΔH" is the relative enthalpy change during the thermal denaturation; "ΔG_D^o" is the relative change in Gibbs free-energy during the chemical denaturation; "$D_{1/2}$" is the guanidine HCl concentration at which the midpoint of chemical denaturation is achieved; "m" is the slope at the midtransition point of chemical denaturation; and "fold increase" is the increase in ANS fluorescence in the presence of the protein relative to free ANS in the same buffer.

[a] Fold increase in signal compared with unbound ANS.

[b] $P < 0.0001$.

[c] $P < 0.005$.

[d] $P < 0.05$.

[e] $P = 0.001$.

[f] $P < 0.0005$.

the thermal denaturation is dependent on the particular unfolding pathway utilized during heat denaturation should not be ruled out.

Finally, although the four mutated amino acids in the apoA-I[218–222] mutants correspond to ~5% of total hydrophobic amino acids of the protein, introduction of the mutations resulted in a 40% reduction of hydrophobic surface exposure, indicating that the residues L218/L219/V221/L222 give rise to almost half of the exposed hydrophobic sites of apoA-I. Taken as a whole, these findings suggest that the apoA-I[218–222] mutant greatly affects the structural integrity and conformational plasticity of apoA-I, effects that may at least partially underlie the observed changes in its in vitro and in vivo functions. The changes in the physicochemical properties of the apoA-I[E223A/K226A] mutant included a 4.2% decrease in its α-helical content, a less cooperative thermal and chemical unfolding, and a 160% increase in the hydrophobic surface exposed to the solvent. These changes indicate that this mutant is thermodynamically destabilized and distinct from the apoA-I[218–222] mutant.

Ability of the apoA-I[218–222] and apoA-I[E223A/K226A] mutants to promote biogenesis of HDL

Adenovirus-mediated gene transfer of the WT apoA-I and apoA-I[218–222] mutant in apoA-I$^{-/-}$ mice showed that, at comparable levels of gene expression, the plasma cholesterol and apoA-I levels of mice expressing apoA-I[218–222] mutant were greatly reduced as compared with WT apoA-I. The plasma cholesterol reduction was due to the great decrease in the HDL cholesterol levels as determined by FPLC fractionation. Density gradient ultracentrifugation of plasma showed that, compared with WT apoA-I, the apoA-I[218–222] mutant was mainly distributed in the HDL3 fraction and its quantity was greatly reduced. The HDL fraction also contained substantial amount of mouse apoE and some apoA-IV.

A sensitive analysis that can detect abnormalities in the pathway of HDL biogenesis is the two-dimensional gel electrophoresis of plasma. This analysis showed that the apoA-I[218–222] mutant when expressed in apoA-I$^{-/-}$ mice generated pre-β- and α4-HDL particles. Such particles were shown previously to undergo fast catabolism by the kidney (11, 34). The ability of the apoA-I[218–222] mutant to form HDL particles was also assessed by EM analysis of the HDL fractions obtained by density gradient ultracentrifugation of plasma. This analysis showed the presence of spherical HDL particles.

We showed recently that apoE- or apoA-IV-containing HDL particles can be formed following a pathway similar to that used for the generation of apoA-I-containing HDL particles (28, 35). Since the HDL fractions 6 and 7 analyzed by EM contained both apoA-I[218–222] mutant and mouse apoE, we considered the possibility that the observed spherical HDL particles in Fig. 2F might represent a mixture of apoA-I- and apoE-containing HDL.

To address this question, we performed gene transfer of the apoA-I[218–222] mutant in double-deficient (apoA-I$^{-/-}$ × apoE$^{-/-}$) mice, which lack the two endogenous mouse apolipoproteins. Density gradient ultracentrifugation showed that the plasma of these mice contained only small amounts of apoA-I in the HDL3 and the lipoprotein-free ($d \geq 1.21$ g/ml) fractions. EM analysis showed the presence of few discoidal HDL as well as spherical particles corresponding in size to LDL and IDL. This is compatible with the presence of apoB-48 and apoA-IV in the HDL density range. Two-dimensional gel electrophoresis of plasma showed that it contained only pre-β-HDL. These data indicated that in apoA-I$^{-/-}$ × apoE$^{-/-}$ mice, the apoA-I[218–222] mutant caused a defective lipidation of apoA-I, possibly due to defective apoA-I/ABCA1 interaction, which resulted in the generation of only pre-β-HDL particles that could not be converted to mature α-HDL particles. Previous studies showed that C-terminal deletion mutants that remove the 220-231 region of apoA-I prevented the biogenesis of normal α-HDL particles but allowed the formation of pre-β-HDL particles (1, 15). Similar pre-β-HDL particles have been found in the plasma of ABCA1-deficient mice and humans carrying ABCA1 mutations that are characterized by HDL deficiency (36–38).

It appears that in apoA-I$^{-/-}$ mice, the diminished interactions between ABCA1 and the apoA-I[218–222] mutant observed in vitro give the opportunity to the mouse apoE to compete more effectively for the ABCA1 binding site (3) and thus to be lipidated. This will lead to the formation of spherical apoE-containing HDL particles that float in the HDL2/HDL3 regions (Fig. 2C, F and supplementary Fig. I). Through unknown mechanisms, the formation of apoE-containing HDL appears to partially stabilize the limited number of nascent HDL particles that contain the apoA-I[218–222] mutant. In the absence of both apoA-I and apoE in the double-deficient mice, there is limited lipidation of the apoA-I[218–222] mutant, as evidenced by the low amount of apoA-I that floats in the HDL region and the formation of few discoidal HDL particles (Fig. 3F, G). The absence of apoE in this case appears to have a major destabilizing effect on any nascent HDL particle formed that contains the apoA-I[218–222] mutant. This explains the low apoA-I and HDL levels and the formation of few discoidal HDL particles associated with this mutant. Furthermore, the absence of apoE allows formation of apoA-IV-containing HDL particles in mice expressing the apoA-I[218–222] mutant that appear to interact with apoB-containing lipoproteins and shift their flotation in the HDL density range.

To explain why α4-HDL particles are formed in the apoA-I$^{-/-}$-deficient mice expressing the apoA-I[218–222] mutant, we explored the possibility of changes in ABCA1 protein or mRNA levels in these mouse models. Previous in vitro experiments had shown that, in THP-1 cells, apoA-I protects ABCA1 from proteasome-mediated degradation (39). However, the in vivo animal experiments in the present study did not show significant changes in ABCA1 mRNA or protein levels in apoA-I$^{-/-}$ or apoA-I$^{-/-}$ × apoE$^{-/-}$ mice without any treatment or following gene transfer of either the WT apoA-I or the apoA-I[218–222] mutant (supplementary Fig. III).

The gene transfer studies with the apoA-I[E223A/K226A] mutant showed that, at similar level of gene expression, the plasma apoA-I levels and the EM profile were comparable to those of WT apoA-I. The HDL was shifted toward the HDL3 region and the total HDL cholesterol levels for this mutant were two thirds of that obtained from apoA-I$^{-/-}$ mice expressing WT apoA-I. Slight differences were also observed in the two-dimensional pattern of this mutant, including increased ratio of pre-β- to α-HDL particles and decreased α1-HDL particles. The in vitro experiments showed that the apoA-I[E223A/K226A] mutant is thermodynamically destabilized, has normal capacity to activate ABCA1, and has a modest reduction (65%) in its capacity to activate LCAT. Overall, the data suggest that the apoA-I[E223A/K226A] mutant had small but distinct effects on the properties of apoA-I and the biogenesis of HDL.

In previous studies, we showed that, when expressed in mouse models, naturally occurring point mutations in apoA-I insufficiently activate LCAT and lead to the accumulation of discoidal HDL particles in plasma. In this category belongs the apoA-I variants apoA-I[R151C]$_{Paris}$ and apoA-I[R160L]$_{Oslo}$ as well as the bioengineered mutants apoA-I[R149A] and apoA-I[R160V/H162A] (11, 13). Other naturally occurring apoA-I variants, such as apoA-I[L141R]$_{Piza}$ and apoA-I[L159R]$_{Finland}$ mutants, when expressed in mouse models, were characterized by very low levels of HDL cholesterol, few HDL particles, and the presence of pre-β- and α4-HDL particles in plasma (12). A characteristic feature of these two categories of mutants, which are associated with low plasma HDL levels, is that the abnormal HDL phenotype could be corrected in vivo by gene transfer of human LCAT (11–13). The phenotype produced by the apoA-I[218–222] mutant is distinct from all previously described phenotypes and cannot be corrected by overexpression of LCAT. In addition, the mutant protein had reduced capability to promote the ABCA1-mediated cholesterol efflux. Although other interpretations are possible, the in vivo and in vitro data suggest that the interaction of the apoA-I[218–222] mutant with ABCA1 results in defective lipidation, which leads to the generation of pre-β-HDL particles that are not a good substrate for LCAT. If this interpretation is correct, one can envision a very precise initial orientation of the apoA-I ligand within the binding site of ABCA1 (3), similar to that described before for enzyme substrate interactions. A precise fit of the apoA-I ligand into the ABCA1 binding site will allow its correct lipidation. The nascent particle thus formed can then undergo cholesterol esterification by LCAT, which leads to the formation of mature α-HDL particles. In contrast, incorrectly lipidated apoA-I becomes a poor substrate of LCAT.

Clinical implications

The apoA-I[218–222] mutant generated a unique aberrant HDL phenotype that has not been observed previously. The hallmark of this phenotype is low HDL levels, formation of pre-β-HDL and discoidal HDL that do not mature to spherical α-HDL particles, and the presence of IDL- and LDL-sized particles in the HDL region that are enriched in apoA-IV and apoB-48. Phenotypes generated by mutagenesis of apoA-I can facilitate the identification of similar phenotypes that may exist in the human population. Such phenotypes may serve in the diagnosis, prognosis, and potential treatment of specific dyslipidemias.

Panagiotis Fotakis, Andreas Kateifides, and Melissa Beck have been students of the graduate program "The Molecular Basis of Human Disease" of the University of Crete Medical School. The authors thank Gayle Forbes for technical assistance. She passed away on September 21, 2013. This article is dedicated to her memory.

REFERENCES

1. Chroni, A., T. Liu, I. Gorshkova, H. Y. Kan, Y. Uehara, A. von Eckardstein, and V. I. Zannis. 2003. The central helices of apoA-I can promote ATP-binding cassette transporter A1 (ABCA1)-mediated lipid efflux. Amino acid residues 220–231 of the wild-type apoA-I are required for lipid efflux in vitro and high density lipoprotein formation in vivo. *J. Biol. Chem.* **278:** 6719–6730.
2. Liu, T., M. Krieger, H. Y. Kan, and V. I. Zannis. 2002. The effects of mutations in helices 4 and 6 of apoA-I on scavenger receptor class B type I (SR-BI)-mediated cholesterol efflux suggest that formation of a productive complex between reconstituted high density lipoprotein and SR-BI is required for efficient lipid transport. *J. Biol. Chem.* **277:** 21576–21584.
3. Hassan, H. H., M. Denis, D. Y. Lee, I. Iatan, D. Nyholt, I. Ruel, L. Krimbou, and J. Genest. 2007. Identification of an ABCA1-dependent phospholipid-rich plasma membrane apolipoprotein A-I binding site for nascent HDL formation: implications for current models of HDL biogenesis. *J. Lipid Res.* **48:** 2428–2442.
4. Zannis, V. I., A. Chroni, K. E. Kypreos, H. Y. Kan, T. B. Cesar, E. E. Zanni, and D. Kardassis. 2004. Probing the pathways of chylomicron and HDL metabolism using adenovirus-mediated gene transfer. *Curr. Opin. Lipidol.* **15:** 151–166.
5. Singaraja, R. R., M. Van Eck, N. Bissada, F. Zimetti, H. L. Collins, R. B. Hildebrand, A. Hayden, L. R. Brunham, M. H. Kang, J. C. Fruchart, et al. 2006. Both hepatic and extrahepatic ABCA1 have discrete and essential functions in the maintenance of plasma high-density lipoprotein cholesterol levels in vivo. *Circulation.* **114:** 1301–1309.
6. Chung, S., J. K. Sawyer, A. K. Gebre, N. Maeda, and J. S. Parks. 2011. Adipose tissue ATP binding cassette transporter A1 contributes to high-density lipoprotein biogenesis in vivo. *Circulation.* **124:** 1663–1672.
7. Kiss, R. S., N. Kavaslar, K. Okuhira, M. W. Freeman, S. Walter, R. W. Milne, R. McPherson, and Y. L. Marcel. 2007. Genetic etiology of isolated low HDL syndrome: incidence and heterogeneity of efflux defects. *Arterioscler. Thromb. Vasc. Biol.* **27:** 1139–1145.
8. Cohen, J. C., R. S. Kiss, A. Pertsemlidis, Y. L. Marcel, R. McPherson, and H. H. Hobbs. 2004. Multiple rare alleles contribute to low plasma levels of HDL cholesterol. *Science.* **305:** 869–872.
9. Frikke-Schmidt, R., B. G. Nordestgaard, G. B. Jensen, and A. Tybjaerg-Hansen. 2004. Genetic variation in ABC transporter A1 contributes to HDL cholesterol in the general population. *J. Clin. Invest.* **114:** 1343–1353.
10. Zannis, V. I., E. E. Zanni, A. Papapanagiotou, D. Kardassis, and A. Chroni. 2006. ApoA-I functions and synthesis of HDL: insights from mouse models of human HDL metabolism. *In* High-Density Lipoproteins. From Basic Biology to Clinical Aspects. Wiley-VCH, Weinheim. 237–265.
11. Koukos, G., A. Chroni, A. Duka, D. Kardassis, and V. I. Zannis. 2007. Naturally occurring and bioengineered apoA-I mutations that inhibit the conversion of discoidal to spherical HDL: the abnormal HDL phenotypes can be corrected by treatment with LCAT. *Biochem. J.* **406:** 167–174.
12. Koukos, G., A. Chroni, A. Duka, D. Kardassis, and V. I. Zannis. 2007. LCAT can rescue the abnormal phenotype produced by the natural ApoA-I mutations (Leu141Arg)Pisa and (Leu159Arg)FIN. *Biochemistry.* **46:** 10713–10721.

13. Chroni, A., A. Duka, H. Y. Kan, T. Liu, and V. I. Zannis. 2005. Point mutations in apolipoprotein a-I mimic the phenotype observed in patients with classical lecithin:cholesterol acyltransferase deficiency. *Biochemistry.* **44:** 14353–14366.
14. Chroni, A., H. Y. Kan, K. E. Kypreos, I. N. Gorshkova, A. Shkodrani, and V. I. Zannis. 2004. Substitutions of glutamate 110 and 111 in the middle helix 4 of human apolipoprotein A-I (apoA-I) by alanine affect the structure and in vitro functions of apoA-I and induce severe hypertriglyceridemia in apoA-I-deficient mice. *Biochemistry.* **43:** 10442–10457.
15. Chroni, A., G. Koukos, A. Duka, and V. I. Zannis. 2007. The carboxy-terminal region of apoA-I is required for the ABCA1-dependent formation of alpha-HDL but not prebeta-HDL particles in vivo. *Biochemistry.* **46:** 5697–5708.
16. Borhani, D. W., D. P. Rogers, J. A. Engler, and C. G. Brouillette. 1997. Crystal structure of truncated human apolipoprotein A-I suggests a lipid-bound conformation. *Proc. Natl. Acad. Sci. USA.* **94:** 12291–12296.
17. Borhani, D. W., J. A. Engler, and C. G. Brouillette. 1999. Crystallization of truncated human apolipoprotein A-I in a novel conformation. *Acta Crystallogr. D Biol. Crystallogr.* **55:** 1578–1583.
18. Mei, X., and D. Atkinson. 2011. Crystal structure of C-terminal truncated apolipoprotein A-I reveals the assembly of high density lipoprotein (HDL) by dimerization. *J. Biol. Chem.* **286:** 38570–38582.
19. Segrest, J. P., L. Li, G. M. Anantharamaiah, S. C. Harvey, K. N. Liadaki, and V. Zannis. 2000. Structure and function of apolipoprotein A-I and high-density lipoprotein. *Curr. Opin. Lipidol.* **11:** 105–115.
20. Ohnsorg, P. M., L. Rohrer, D. Perisa, A. Kateifides, A. Chroni, D. Kardassis, V. I. Zannis, and A. von Eckardstein. 2011. Carboxyl terminus of apolipoprotein A-I (ApoA-I) is necessary for the transport of lipid-free ApoA-I but not prelipidated ApoA-I particles through aortic endothelial cells. *J. Biol. Chem.* **286:** 7744–7754.
21. Biedzka-Sarek, M., J. Metso, A. Kateifides, T. Meri, T. S. Jokiranta, A. Muszynski, J. Radziejewska-Lebrecht, V. Zannis, M. Skurnik, and M. Jauhiainen. 2011. Apolipoprotein A-I exerts bactericidal activity against Yersinia enterocolitica serotype O:3. *J. Biol. Chem.* **286:** 38211–38219.
22. Amar, M. J., R. D. Shamburek, B. Vaisman, C. L. Knapper, B. Foger, R. F. Hoyt, Jr., S. Santamarina-Fojo, H. B. Brewer, Jr., and A. T. Remaley. 2009. Adenoviral expression of human lecithin-cholesterol acyltransferase in nonhuman primates leads to an antiatherogenic lipoprotein phenotype by increasing high-density lipoprotein and lowering low-density lipoprotein. *Metabolism.* **58:** 568–575.
23. Matz, C. E., and A. Jonas. 1982. Micellar complexes of human apolipoprotein A-I with phosphatidylcholines and cholesterol prepared from cholate-lipid dispersions. *J. Biol. Chem.* **257:** 4535–4540.
24. Williamson, R., D. Lee, J. Hagaman, and N. Maeda. 1992. Marked reduction of high density lipoprotein cholesterol in mice genetically modified to lack apolipoprotein A-I. *Proc. Natl. Acad. Sci. USA.* **89:** 7134–7138.
25. Thorngate, F. E., P. G. Yancey, G. Kellner-Weibel, L. L. Rudel, G. H. Rothblat, and D. L. Williams. 2003. Testing the role of apoA-I, HDL, and cholesterol efflux in the atheroprotective action of low-level apoE expression. *J. Lipid Res.* **44:** 2331–2338.
26. Zhang, S. H., R. L. Reddick, J. A. Piedrahita, and N. Maeda. 1992. Spontaneous hypercholesterolemia and arterial lesions in mice lacking apolipoprotein E. *Science.* **258:** 468–471.
27. Chroni, A., H. Y. Kan, A. Shkodrani, T. Liu, and V. I. Zannis. 2005. Deletions of helices 2 and 3 of human apoA-I are associated with severe dyslipidemia following adenovirus-mediated gene transfer in apoA-I-deficient mice. *Biochemistry.* **44:** 4108–4117.
28. Duka, A., P. Fotakis, D. Georgiadou, A. Kateifides, K. Tzavlaki, L. von Eckardstein, E. Stratikos, D. Kardassis, and V. I. Zannis. 2013. ApoA-IV promotes the biogenesis of apoA-IV-containing HDL particles with the participation of ABCA1 and LCAT. *J. Lipid Res.* **54:** 107–115.
29. Kateifides, A. K., I. N. Gorshkova, A. Duka, A. Chroni, D. Kardassis, and V. I. Zannis. 2011. Alteration of negatively charged residues in the 89 to 99 domain of apoA-I affects lipid homeostasis and maturation of HDL. *J. Lipid Res.* **52:** 1363–1372.
30. Rothblat, G. H., M. Llera-Moya, V. Atger, G. Kellner-Weibel, D. L. Williams, and M. C. Phillips. 1999. Cell cholesterol efflux: integration of old and new observations provides new insights. *J. Lipid Res.* **40:** 781–796.
31. Fielding, C. J., and P. E. Fielding. 2001. Cellular cholesterol efflux. *Biochim. Biophys. Acta.* **1533:** 175–189.
32. Wang, N., D. L. Silver, P. Costet, and A. R. Tall. 2000. Specific binding of ApoA-I, enhanced cholesterol efflux, and altered plasma membrane morphology in cells expressing ABC1. *J. Biol. Chem.* **275:** 33053–33058.
33. Remaley, A. T., J. A. Stonik, S. J. Demosky, E. B. Neufeld, A. V. Bocharov, T. G. Vishnyakova, T. L. Eggerman, A. P. Patterson, N. J. Duverger, S. Santamarina-Fojo, et al. 2001. Apolipoprotein specificity for lipid efflux by the human ABCAI transporter. *Biochem. Biophys. Res. Commun.* **280:** 818–823.
34. Timmins, J. M., J. Y. Lee, E. Boudyguina, K. D. Kluckman, L. R. Brunham, A. Mulya, A. K. Gebre, J. M. Coutinho, P. L. Colvin, T. L. Smith, et al. 2005. Targeted inactivation of hepatic Abca1 causes profound hypoalphalipoproteinemia and kidney hypercatabolism of apoA-I. *J. Clin. Invest.* **115:** 1333–1342.
35. Kypreos, K. E., and V. I. Zannis. 2007. Pathway of biogenesis of apolipoprotein E-containing HDL in vivo with the participation of ABCA1 and LCAT. *Biochem. J.* **403:** 359–367.
36. Daniil, G., A. A. Phedonos, A. G. Holleboom, M. M. Motazacker, L. Argyri, J. A. Kuivenhoven, and A. Chroni. 2011. Characterization of antioxidant/anti-inflammatory properties and apoA-I-containing subpopulations of HDL from family subjects with monogenic low HDL disorders. *Clin. Chim. Acta.* **412:** 1213–1220.
37. Francone, O. L., P. V. Subbaiah, A. van Tol, L. Royer, and M. Haghpassand. 2003. Abnormal phospholipid composition impairs HDL biogenesis and maturation in mice lacking Abca1. *Biochemistry.* **42:** 8569–8578.
38. Asztalos, B. F., M. E. Brousseau, J. R. McNamara, K. V. Horvath, P. S. Roheim, and E. J. Schaefer. 2001. Subpopulations of high density lipoproteins in homozygous and heterozygous Tangier disease. *Atherosclerosis.* **156:** 217–225.
39. Arakawa, R., and S. Yokoyama. 2002. Helical apolipoproteins stabilize ATP-binding cassette transporter A1 by protecting it from thiol protease-mediated degradation. *J. Biol. Chem.* **277:** 22426–22429.